J Fluoresc (2011) 21:1111–1115
DOI 10.1007/s10895-010-0786-y

ORIGINAL PAPER

On the Luminescence of Ce^{3+}, Eu^{3+}, and Tb^{3+} in Novel Borate $LiSr_4(BO_3)_3$

Xinmin Zhang · Haiyan Lang · Hyo Jin Seo

Received: 6 September 2010 / Accepted: 28 November 2010 / Published online: 9 December 2010

Abstract This paper reports on the photoluminescence (PL) and time-resolved properties of Ce^{3+}, Eu^{3+}, and Tb^{3+} in novel $LiSr_4(BO_3)_3$ powder phosphors. Ce^{3+} shows an emission band peaking at 420 nm under 350-nm UV excitation. Energy transfer from Ce^{3+} to Mn^{2+} takes place in the co-doped samples. Eu^{3+} shows red emission under near UV excitation. $LiSr_4(BO_3)_3$:Eu^{3+} phosphor could be a suitable candidate for phosphor-converted solid state lighting. The luminescence lifetime is 2.13 ms for Eu^{3+} in $LiSr_4(BO_3)_3$:0.001Eu^{3+}. As Eu^{3+} concentration increasing, the decay curves deviate from exponential behavior. Tb^{3+} shows the strongest $^5D_4 \rightarrow {}^7F_5$ emission line at 540 nm. Decay curves of $^5D_4 \rightarrow {}^7F_5$ and $^5D_3 \rightarrow {}^7F_5$ emission with different Tb^{3+} concentrations were also measured. Cross-relaxation process is discussed based on the decay curves.

Keywords Phosphor · Luminescence · Decay curve · Borate

Introduction

Rare earths and transition metal ion doped phosphors have attracted more attention due to their extensive applications in the fields of lighting, display and medical science as well as fundamental studies [1–6]. Phosphors are usually made from a suitable host material, to which an activator is added. The well known host materials are oxides [7], nitrides and oxynitrides [1, 8, 9], sulfides, phosphates [10], halides [11], silicates [12, 13] and borates. Among the borates based phosphors, $InBO_3$:Eu, $InBO_3$:Tb, $Sr_6P_5BO_{20}$:Eu, SrB_4O_7:Eu and $SrFB_2O_3$:Eu(II) have been utilized in industry [14]. Recently, borates based phosphors have been studied due to their lower synthesis temperature and other advantages [15–21]. The compound, $MM'_4(BO_3)_3$ (M = Li, Na, K; M' = Ca, Sr, Ba), represents a new structure type [22, 23]. Jiang and his co-workers have reported the thermoluminescence characteristics of $NaSr_4(BO_3)_3$:Ce^{3+} [24], $LiSr_4(BO_3)_3$:Ce^{3+} [25], and $KSr_4(BO_3)_3$:Ce^{3+} [26] phosphors. In the former papers we reported on the photoluminescence properties of $NaCa_4(BO_3)_3$:Eu^{3+} and $NaSr_4(BO_3)_3$:Ce^{3+}, Mn^{2+} [27, 28]. Theses materials emit intense visible light and are promising phosphors for practical application. Among these compounds, $LiSr_4(BO_3)_3$ crystallizes in the cubic space group $Ia\bar{3}d$ with large lattice parameters: a=14.95066(5) Å. In this paper, the luminescence and time-resolved properties of Ce^{3+}, Eu^{3+}, and Tb^{3+} in $LiSr_4(BO_3)_3$ are described in detail.

Experimental

Samples of $LiSr_4(BO_3)_3$:RE (RE=Ce^{3+}, Eu^{3+}, Tb^{3+}) were prepared according to the standard solid-state technique. High-purity starting materials Li_2CO_3 (Aldrich, 99.9%), $SrCO_3$ (Aldrich, 99.9%), H_3BO_3 (Aldrich, 99.9%, 10 mol% excess to compensate the evaporation in the heating processes), Eu_2O_3 (Aldrich, 99.99%), Tb_4O_7 (Aldrich, 99.99%), and CeO_2 (Aldrich, 99.99%) were used. The well mixed materials were pre-sintered at 500°C for 3 h, then

X. Zhang · H. Lang
School of Materials Science and Engineering, Central South University of Forestry and Technology, Changsha 410004, China

H. Jin Seo (✉)
Department of Physics, Pukyong National University, Busan 608-737, Republic of Korea
e-mail: hjseo@pknu.ac.kr

annealed at 800°C for 12 h in air (for Eu^{3+} doped samples) or weak CO reducing atmosphere (for Tb^{3+}, Ce^{3+} doped samples) with an intermediate grinding. Li_2CO_3 was added as a charge compensator. The structural characteristics of $LiSr_4(BO_3)_3$:RE samples were checked by X-ray diffraction (XRD) patterns using a Rigaku D/max 2200 Diffractometer with Cu Kα radiation at 40 kV, 30 mA. All the samples are single phase. The PL emission and excitation spectra were measured by Fluorolog-3 Fluorescence Spectrophotometer with 450 W Xenon lamps. The luminescence decays were measured by monitoring the given emission from the samples under 266 nm pulsed laser excitation. Decay profiles were recorded by the 500 MHz digital oscilloscope (LeCroy 9350A) in which the signal was fed from PMT.

Results and Discussion

The PL excitation and emission spectra of $LiSr_4(BO_3)_3$:0.01 Ce^{3+} are given in Fig. 1. Either 410 or 460 nm emission are monitored, the excitation spectra are similar to each other and consist of two distinct broad-bands peaking at about 280 and 340 nm. The absorption bands are assigned to the crystal field levels of the 4*f*5*d* states for Ce^{3+}, and the lowest 5*d*-level absorption for Ce^{3+} in $LiSr_4(BO_3)_3$ is about 3.65 eV (340 nm). Under 350-nm UV excitation PL emission spectrum shows an asymmetry emission band peaking at 420 nm. The luminescence is ascribed to a 5*d*-4*f* transition on Ce^{3+}, corresponding to the transitions of 5*d* excited state to $^2F_{5/2}$ and $^2F_{7/2}$ ground states.

It is well known that the transitions of Mn^{2+} are spin and parity forbidden; the emission and excitation intensities are often weak under UV light excitation. Ce^{3+} can absorb UV light, especially the near-UV in some matrixes. Many authors have reported that Mn^{2+} emission can be strengthened by means of energy transfer from Ce^{3+} to Mn^{2+} [3, 29–31]. In these cases, a significant spectral overlap between the emission peak of Ce^{3+} and the excitation peak of Mn^{2+} ($^6A_1 \rightarrow {}^4A_1$, ^4E transition) has been observed, indicating that efficient resonance-type energy transfer from Ce^{3+} to Mn^{2+} takes place. Based on the Ce^{3+} emission in $LiSr_4(BO_3)_3$ matrix, we also studied the possibility of $Ce^{3+} \rightarrow Mn^{2+}$ energy transfer in Ce^{3+}, Mn^{2+} co-doped phosphors. The PL excitation and emission spectra of $LiSr_4(BO_3)_3$:0.04Ce^{3+},0.16Mn^{2+} sample are shown in Fig. 2. It can be seen that the emission spectrum exhibits a strong blue band (420 nm) and a weak red band (600 nm). The two bands are attributed to the *d*→*f* transition of Ce^{3+} and $^4T_1$-$^6A_1$ transition of Mn^{2+}, respectively. For the Mn^{2+} single dopant sample, the Mn^{2+} emission is too weak to be observed because of forbidden transition. So the red band emission of Mn^{2+} ions in co-doped sample should be attributed to the energy transfer from Ce^{3+} to Mn^{2+}. Unfortunately, the transfer efficiency is not satisfactory. The excitation spectra of the 420 and 600 nm emission correspond to the *f*→*d* transitions in the Ce^{3+} ion, which also confirms the energy transfer taking place between Ce^{3+} and Mn^{2+} ions.

Eu^{3+} doped $LiSr_4(BO_3)_3$ phosphors show red emission under UV excitation. Figure 3 shows the PL excitation and emission spectra of $LiSr_4(BO_3)_3$:1.0Eu^{3+}. Under 260 and 393 nm excitation, the Eu^{3+} emission consists of the well-known transitions from the $^5D_0$ to ^7F_J levels. The emission peaks observed at 578, (585, 595), 613, 650, and (685, 700) nm are assigned to the transitions $^5D_0 \rightarrow {}^7F_0$, $^5D_0 \rightarrow {}^7F_1$, $^5D_0 \rightarrow {}^7F_2$, $^5D_0 \rightarrow {}^7F_3$, and $^5D_0 \rightarrow {}^7F_4$, respectively. Moreover, the red light emission does not quench even if the *x* value is up to 1.0 in $LiSr_4(BO_3)_3$:*x*Eu^{3+} system. The excitation spectrum (λ_{em}=613 nm) consists of broad excitation band peaking at about 260 nm and some intense *f*→*f* absorption lines. The excitation band should be assigned to the charge transfer transition from O^{2-} to Eu^{3+} in the host lattice. The absorption of BO_3 groups may be situated at higher energy level [32, 33]. The sharp lines in the 300~550 nm range are intraconfigurational 4*f*-4*f* transition of Eu^{3+} ions in the host

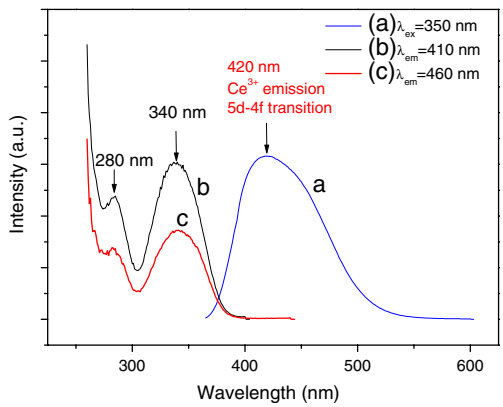

Fig. 1 Emission (**a**) and excitation (**b** and **c**) spectra of the luminescence of $LiSr_4(BO_3)_3$:0.01Ce^{3+}

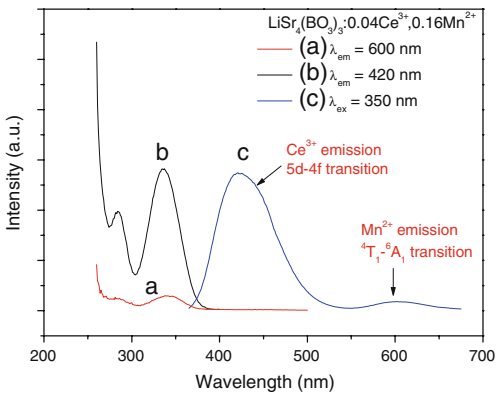

Fig. 2 Excitation (**a** and **b**) and emission (**c**) spectra of the luminescence of $LiSr_4(BO_3)_3$:0.04Ce^{3+},0.16Mn^{2+}

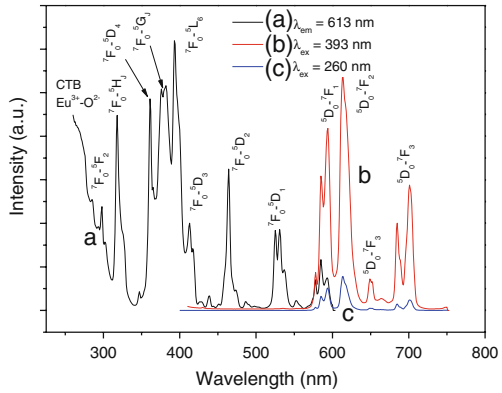

Fig. 3 Excitation (**a**) and emission (**b**) spectra of the luminescence of $LiSr_4(BO_3)_3$:1.0Eu^{3+}

lattices. It is noted that the phosphors exhibit intense absorption around 400 nm, and this absorption band match the emission of near UV InGaN chip; so $LiSr_4(BO_3)_3$:Eu^{3+} phosphor could be a suitable candidate for phosphor-converted solid state lighting.

When the luminescent centers have different local environments, the associated ions relax at different rates [34, 35]. The decay curves of $^5D_0 \rightarrow {}^7F_2$ emission for $LiSr_4(BO_3)_3$ doped with different Eu^{3+} concentrations ($0.001 \le x \le 1.0$) under excitation at 266 nm are shown in Fig. 4. It can be seen that the decay curves are single exponential when $x \le 0.04$. The luminescence lifetime derived from the fitted curves are 2.13 ms for Eu^{3+} in $LiSr_4(BO_3)_3$:0.001Eu^{3+}. As Eu^{3+} concentration increases, the decay curves deviate from exponential behavior, and the non-exponential change becomes more prominent with increasing Eu^{3+} content, which indicates that more than one relaxation process exists. With the Eu^{3+} concentration increasing, the distances between Eu^{3+} ions shorten; then the probability of an energy transfer among Eu^{3+} ions becomes more frequent. The mechanism of energy transfer is under investigation.

The PL emission and excitation spectra of $LiSr_4(BO_3)_3$:0.08 Tb^{3+} phosphor are shown in Fig. 5. In the excitation spectrum of the $^5D_4 \rightarrow {}^7F_5$ transition (540 nm), the sharp absorption lines at 317, 351, 367, 377, and 485 nm are due to the transitions from $^7F_6$ to ^5D_J, ^5G_J, $^5L_{10}$, $^5D_3$, and $^5D_4$, respectively. The absorption band peaking at 280 nm can be ascribed to the $4f^8 \rightarrow 4f^7 5d^1$ transition of Tb^{3+} ion. Tb^{3+} ion with $4f^8$ configuration has complicated energy levels, so luminescence spectrum consisting of many lines due to $^5D_J \rightarrow {}^7F_J$ is observed. In this case, the emission spectrum shows the strongest $^5D_4 \rightarrow {}^7F_5$ emission line at approximately 540 nm. Moreover, the $^5D_3$ emission is weaker than that of $^5D_4$ emission even in the sample with very low Tb^{3+} concentration ($LiSr_4(BO_3)_3$:0.001 Tb^{3+}), and it does not disappear even with higher Tb^{3+} concentration ($LiSr_4(BO_3)_3$:0.20 Tb^{3+}).

The decay curves of $^5D_3 \rightarrow {}^7F_5$ emission (415 nm) for $LiSr_4(BO_3)_3$ doped with different Tb^{3+} concentrations under excitation at 266 nm are shown in Fig. 6. A double exponential decay behavior of the luminescence emission has been observed. All the decay curves can fit very well to a double exponential function. The short lifetime is about 1 μs and decreases with increasing Tb^{3+} concentration. The fast decay component may be attributed to the host lattice emission or some kind of Tb^{3+} cluster or pair [36]. The slow decay component can be ascribed to the $^5D_3 \rightarrow {}^7F_5$ transition of Tb^{3+}. There is no obvious change to the lifetime of this transition, and the fitted lifetime is about 40 μs.

Figure 7 shows the decay curves of $^5D_4 \rightarrow {}^7F_5$ emission (540 nm) for $LiSr_4(BO_3)_3$ doped with different Tb^{3+} concentrations under excitation at 266 nm. It can be seen that the decay curves show a nearly single exponential decay for those samples with lower Tb^{3+} concentration

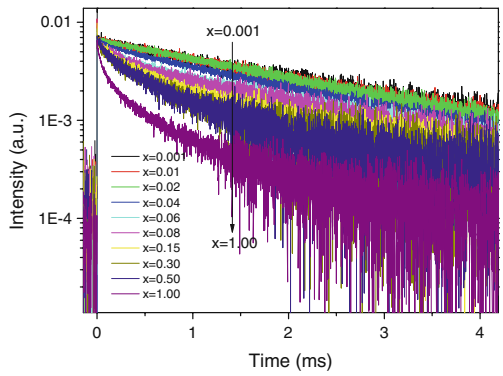

Fig. 4 Decay curves of $^5D_0 \rightarrow {}^7F_2$ emission for $LiSr_4(BO_3)_3$ doped with different Eu^{3+} concentrations under excitation at 266 nm. The signals were detected at 616 nm

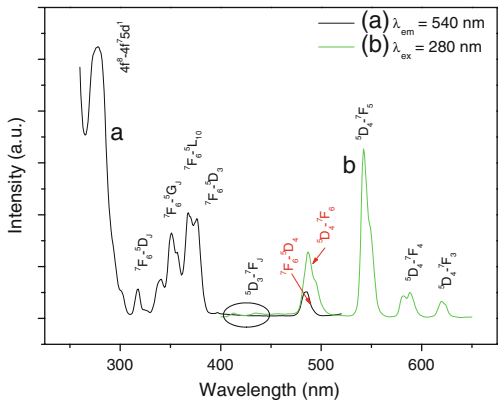

Fig. 5 Excitation (**a**) and emission (**b**) spectra of the luminescence of $LiSr_4(BO_3)_3$:0.08 Tb^{3+}

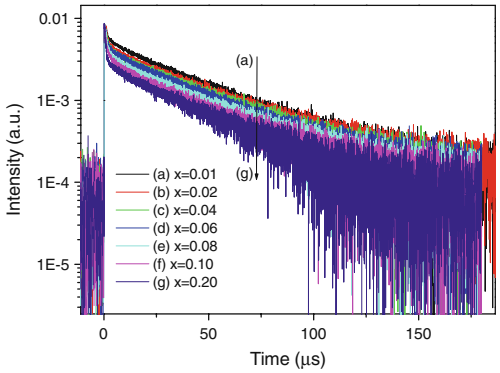

Fig. 6 Decay curves of $^5D_3 \rightarrow {}^7F_5$ emission for $LiSr_4(BO_3)_3$ doped with different Tb^{3+} concentrations under excitation at 266 nm. The signals were detected at 415 nm

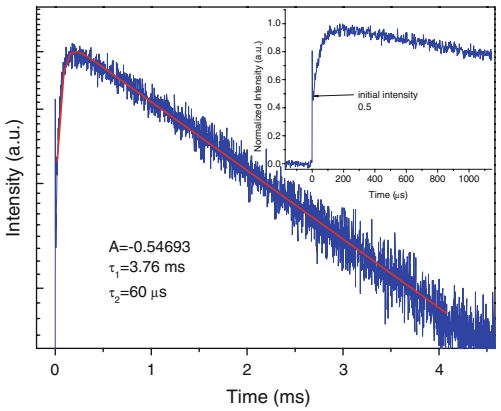

Fig. 8 Simulated decay curve of using equation (1) for $LiSr_4(BO_3)_3$:0.01 Tb^{3+} phosphor (the inset shows the initial intensity of $^5D_4 \rightarrow {}^7F_5$ transition)

(e.g., x=0.01 and 0.02). A single exponential fit derives a decay time about 3.6 ms. It is also noted that the decay curves (curves a and b) exhibit an initial rise phenomenon (marked with black circle in Fig. 7). We attempted to fit these curves with double exponential equation [37, 38]:

$$I(t) = I_0\left[\exp\left(\frac{-t}{\tau_1}\right) + A\exp\left(\frac{-t}{\tau_2}\right)\right] \quad (1)$$

Where, I and I_0 is the luminescence intensity, t is the time, τ_1 is a decay time, τ_2 is a decay and/or rise time, A is the ratio of the two parts of the function. When $A<0$, the second term represents rising, and for $A>0$, the second term represents a further decay. The results of the fitting indicate that the best agreement between experimental data and theoretical fits is obtained, and the result of $LiSr_4(BO_3)_3$:0.01 Tb^{3+} sample is shown in Fig. 8. The values of parameters are τ_1=3.76 ms (decay time), τ_2=60 μs (rise time) and A= −0.54693. The rise time of 60 μs is close to the value of the decay time of the $^5D_3$ emission in this matrix, indicating the initial slow rise is attributed to the $^5D_3 \rightarrow {}^5D_4$ cross-relaxation process. The initial intensity of 0.5 represents about 50% of $^5D_4$ population feeding directly from the 5*d* level and 50% population feeding from higher energy level ($^5D_3$) of Tb^{3+} by cross-relaxation process [39]. For $x \geq 0.04$, the decay curves become nonexponential due to the radiationless process involving Tb^{3+} ions [36], and the mechanism is under investigation. The initial rise part disappears quickly, which may be due to the higher Tb^{3+} concentration [36].

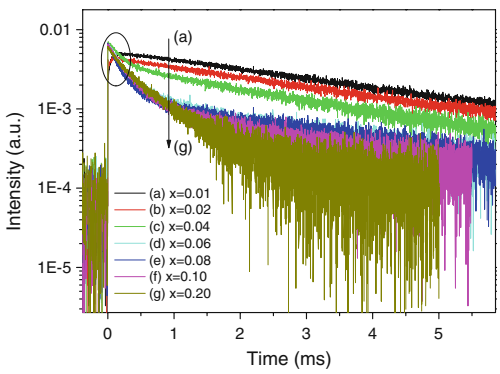

Fig. 7 Decay curves of $^5D_4 \rightarrow {}^7F_5$ emission for $LiSr_4(BO_3)_3$ doped with different Tb^{3+} concentrations under excitation at 266 nm. The signals were detected at 540 nm

Conclusions

In summary, we have reported on the synthesis and PL properties of Ce^{3+}, Eu^{3+}, and Tb^{3+} in novel $LiSr_4(BO_3)_3$ powder phosphors. The $LiSr_4(BO_3)_3$:Ce^{3+} phosphor shows a blue emission peaking at 420 nm under excitation by 350 nm UV light. The emission is due to the 5*d*-4*f* transition of Ce^{3+}. In the Ce^{3+}, Mn^{2+} co-doped samples energy transfer from Ce^{3+} to Mn^{2+} occurs. The $LiSr_4(BO_3)_3$:Eu^{3+} phosphor shows red emission under near UV excitation. $LiSr_4(BO_3)_3$:Eu^{3+} phosphor could be a potential candidate for phosphor-converted solid state lighting. The decay curves of $LiSr_4(BO_3)_3$:xEu^{3+} phosphors are single exponential when $x \leq 0.04$, and deviate from exponential behavior, with increasing Eu^{3+} content, which indicates that more than one relaxation process exists. The $LiSr_4(BO_3)_3$:Tb^{3+} phosphor shows strongest $^5D_4 \rightarrow {}^7F_5$ emission line at 540 nm. The decay curves of $^5D_3 \rightarrow {}^7F_5$ emission can be fitted well by double exponential function. The decay curves of $^5D_4 \rightarrow {}^7F_5$ emission exhibit a nearly single exponential decay for those samples with dilute Tb^{3+}

concentration with lifetime of 3.6 ms, and they exhibit an initial rise phenomenon, which is attributed to the $^5D_3 \rightarrow {}^5D_4$ cross-relaxation process.

Acknowledgements This work was supported by the Science and Technology Program of Hunan Province (No. 2010FJ3092). This work was also supported by Mid-career Researcher Program through NRF grant funded by the MEST (No. 2009-0078682).

References

1. Zhu XW, Masubuchi Y, Motohashi T, Kikkawa S (2010) J Alloy Compd 489:157–161
2. Zhou L, Huang J, Gong F, Lan Y, Tong Z, Sun J (2010) J Alloy Compd 495:268–271
3. Zhang X, Seo H-J (2010) Physica B 405:2436–2439
4. Joshi C, Kumar K, Rai S (2010) J Fluoresc 20:953–959
5. Marques A, Tanaka M, Longo E, Leite E, Rosa I (In Press) J Fluoresc
6. Sontakke AD, Biswas K, Mandal A, Annapurna K (2010) J Fluoresc 20:425–434
7. Zhang S, Wang L, Peng H, Li G, Chen K (2010) Mater Chem Phys 123:714–718
8. Yun B-G, Horikawa T, Hanzawa H, Machida K-i (2010) J Electrochem Soc 157:J364–J370
9. Yin L-J, Xu X, Yu W, Yang J-G, Yang L-X, Yang X-F, Hao L-Y, Liu X-J (2010) J Am Ceram Soc 93:1702–1707
10. Zhong J, Liang H, Su Q, Zhou J, Huang Y, Gao Z, Tao Y, Wang J (2010) Appl Phys B 98:139–147
11. Xia Z, Du P, Liao L, Li G, Jin S (2010) Curr Appl Phys 10:1087–1091
12. Zhang XM, Li WL, Shi L, Qiao XB, Seo HJ (2010) Appl Phys B 99:279–284
13. Zhang X, Zhang J, Wang R, Gong M (2010) J Am Ceram Soc 93:1368–1371
14. Shionoya S, Yen WM (1999) Phosphor handbook. CRC Press, New York
15. Zhang X, Qiao X, Seo HJ (2010) J Electrochem Soc 157:J267–J269
16. Zhang H, Wang Y, Tao Y, Li W, Hu D, Feng E, Nie X (2010) J Electrochem Soc 157:J293–J296
17. Yashashchandra D, Shyam Bahadur R (2010) J Am Ceram Soc 93:727–731
18. Yang Y, Yu L, Tao C, Dai Z, Yang H (2010) J Electroceram 25:56–59
19. Xie N, Huang Y, Qiao X, Shi L, Seo HJ (2010) Mater Lett 64:1000–1002
20. Xiao F, Xue YN, Ma YY, Zhang QY (2010) Phys B 405:891–895
21. Xia Z, Du H, Sun J, Chen D, Wang X (2010) Mater Chem Phys 119:7–10
22. Wu L, Chen XL, Li H, He M, Xu YP, Li XZ (2005) Inorg Chem 44:6409–6414
23. Wu L, Chen XL, Xu YP, Sun YP (2006) Inorg Chem 45:3042–3047
24. Jiang L, Zhang Y, Li C, Pang R, Shi L, Zhang S, Hao J, Su Q (2009) J Rare Earths 27:320–322
25. Jiang LH, Zhang YL, Li CY, Hao JQ, Su Q (2007) Mater Lett 61:5107–5109
26. Jiang LH, Zhang YL, Li CY, Hao JQ, Su Q (2009) J Alloy Compd 482:313–316
27. Zhang X, Seo HJ (2010) J Alloy Compd 503:L14–L17
28. Zhang X, Qiao X, Seo HJ (In Press) Curr Appl Phys
29. Yonesaki Y, Takei T, Kumada N, Kinomura N (2010) J Solid State Chem 183:1303–1308
30. Huang C-H, Kuo T-W, Chen T-M (2010) Acs Appl Mater Inter 2:395–1399
31. Xie WJ, Tang JY, Hao LY, Xu X (2009) Opt Mater 32:274–276
32. Dorenbos P (2005) J Lumin 111:89–104
33. Saubat B, Fouassier C, Hagenmuller P, Bourcet JC (1981) Mater Res Bull 16:193–198
34. Lin H-J, Chang Y-S (2007) Electrochem Solid-State Lett 10:J79–J82
35. Seeta Rama Raju G, Park JY, Jung HC, Moon BK, Jeong JH, Kim JH (2009) Curr Appl Phys 9:e92–e95
36. Sohn K-S, Choi YY, Park HD (2000) J Electrochem Soc 147:1988–1992
37. Kondo H, Hirai T, Hashimoto S (2004) J Lumin 108:59–63
38. Zhang XM, Zhang JH, Liang LF, Qiang S (2005) Mater Res Bull 40:281–288
39. Jang KH, Sung WK, Kim ES, Shi L, Jeong JH, Seo HJ (2009) J Lumin 129:1853–1856